International Journal of Automation and Power Engineering, 2012, 1: 151-158
Published Online September 2012

www.ijape.org

Three-phase Probabilistic Load Flow Including Photovoltaic Generation in Distribution System

Ming Ding, Xinglong Wu
Photovoltaic System Research Center of Ministry of Education, Hefei University of Technology, Hefei, China
Email: xinglongwu1988@163.com

(Abstract) This paper presents a method of solving three-phase probabilistic load flow (PLF) for distribution system with single-phase and three-phase grid-connected photovoltaic (PV) systems using the sequential Monte Carlo technique. A novel probabilistic model of output power of PV system is proposed considering random change of weather and hourly variation of relevant parameters. The time-varying load with randomness is also incorporated in PLF. Some cases in modified IEEE 33-node distribution system have been implemented to verify the method. Time-sequence impacts of PV generation on power flow and voltage profiles in distribution system, taking into account the correlation of weather between different zones, are gained from results.

Keywords: Grid-connected Photovoltaic System; Sequential Monte Carlo; Distribution System; Three-phase Probabilistic Load Flow.

Nomenclature

δ	Solar declination angle.
α	Solar altitude angle.
θ	Solar incident angle.
n	Date serial number from Jan. 1st.
φ	Latitude of PV installation site.
L_{loc}	Longitude of PV installation site.
L_{st}	Longitude of where standard time corresponds to.
ω	Hour angle.
t	Local time, i.e. true solar time.
t_{st}	Standard time, refer to Beijing time in this paper.
E	Time difference.
m	Solar air mass.
P	Coefficient of atmospheric transpareney.
P_2	Average annual coefficient of atmospheric transpareney.
G_0	Solar irradiance of exoatmospheric tangential plane.
G_{sc}	Solar constant, defined as 1382W/㎡ generally.
γ	Correction factor of eccentricity from earth to sun.
G_n	Solar direct irradiance through the atmosphere.
G_d	Solar diffuse irradiance through the atmosphere.
t_{rise}, t_{set}	Sunrise time and sunset time.
G	Solar irradiance on the inclined PV arrays.
β	Inclination of PV arrays to the horizontal plane.
L,W	Length and width of PV arrays.
D	Distance between the front and back PV arrays.
R	Number of rows of PV arrays.
ρ	Reflectance of the ground.
T	Temperature of PV cells.
T_a	Air temperature.
η	Efficiency of PV cells.
η_o	Efficiency of PV cells at reference temperature.
T_r	Reference temperature, 25℃ or 298K.
ε	Temperature coefficient of PV arrays.
P_s	Ratio of shadow.
S	Effective sun light area of PV arrays.
η_{inv}	Efficiency of inverter.
η_{mppt}	Efficiency of maximum power point tracking (MPPT).
P_{PV}	Output power of grid-connected PV system.
P_N	Rated power of grid-connected PV system.
U,U_1,U_2	Uniformly distributed random number.
T_{run}	Run time of PV system.
T_{repair}	Repair time of PV system.
λ_{pv}, μ_{pv}	Fault rate and repair rate of PV system.

1. Introduction

There was an increased utilization of photovoltaic (PV) during recent years due to liberalized markets and the global trend of reducing greenhouse gas emissions [1]. The development of PV is promoted by favorable policies all over the world. Chinese governments are also making efforts to encourage the progress of PV. With the development of PV generation technique, more and more PV plants and family-hold single-phase PV systems are connected to distribution networks in China. However, integration of PV generation brings various impacts on load flow, voltage profile, voltage regulation, short-circuit current, protections, et al. in distribution system, since actual distribution networks are designed as radially operated and PV generation changes the single-source network to multi-source one [2-4]. Regarding load flow, the grid-connected PV systems change

its level, direction and distribution. The uncertainty also increases in load flow because the output power of PV systems are random due to variation of solar irradiance and weather. Based on the change of load flow, sometimes the voltage may cross normal limit which means upper limit generally. If there are single-phase PV systems connected to the network, voltage imbalance which is measured by negative sequence voltage unbalance factor (NSVUF) will occur and the NSVUF may be beyond stated limit sometimes. It is unable to evaluate the impact of stochastic change on the operation of distribution system roundly by simply using deterministic load flow analysis which aims at specific input parameters of the network, but the problem is solved via probabilistic load flow (PLF).

Currently, studies of PLF in distribution system with PV generation focus on voltage quality and include two main parts, i.e., the output model of grid-connected PV system and the analysis method of PLF. Some researches assume that the probability density function (PDF) of the output of PV system follows Beta distribution [5] or normal distribution [6] as well as the solar irradiance. In [7] parameters of PV cells and historical weather are used to calculate the output of PV system at 15-minute time step and the sequential output power is obtained. The random nature of hourly clearness index is taken into account and a complex PDF of the output of PV system is yielded in [1] [8] [9], while the random nature of hourly diffuse index is considered as well as hourly clearness index and the PDF of the PV output is gained according to the PDFs of the overall solar irradiance and the diffuse irradiance in [10]. In addition, dynamic random variable is defined in [11] and the probabilistic model of PV output is obtained using superposition of the certain rule and random variable. As far as the analysis method, the PLF can be solved numerically or analytically, so the method of combined cumulants and Gram-Charlier [5] [10] [11] or Cornish-Fisher [9], two-point estimate method [6] and Monte Carlo techniques [1] [7] are used. But PDFs of voltage, mean values of voltage, et al. obtained from these studies are static without time-sequence change except the work in [11]. Moreover, all studies concentrate on three-phase symmetrical distribution system with three-phase grid-connected PV systems, which are not appropriate for unsymmetrical network with single-phase grid-connected PV systems. For example, the voltage imbalance caused by single-phase PV systems can not be analyzed in above studies.

Then, to solve these problems, this paper presents three-phase PLF for distribution system with three-phase and single-phase grid-connected PV systems, using the sequential Monte Carlo simulation. In the procedure, the sequential probabilistic model of PV output power is illustrated in detail considering solar irradiance, random change of weather, efficiency and effective sunlight area of PV arrays, efficiency of MPPT and inverter, and the reliability of overall grid-connected PV systems. Besides, the time-varying model of random loads is also taken into account. The method can be used to provide power flows and voltage profiles at any time during the 24-hour cycle of a specific day and month, and it will be verified to be feasible in modified IEEE 33-node distribution system with three-phase unsymmetrical parameters.

2. Proposed Probabilistic Model of Pv Output Power

The output power of grid-connected PV system relates to the solar irradiance, the conversion efficiency of PV cells, the effective sun light area of PV arrays, the efficiency of MPPT and inverter, et al.

2.1. Model of Solar Irradiance

Solar irradiance includes direct irradiance and diffuse irradiance and changes with different places, seasons and hours. Therefore, solar irradiance is variable for 24 hours in one day, which can be calculated as follows.

2.1.1 Model of solar irradiance under clear sky

The model of solar irradiance under clear sky is regular without the random effect. The declination, altitude angle, solar air mass, coefficient of atmospheric transpareney and solar irradiance of exoatmospheric tangential plane should be calculated.

According to the Cooper equation, the declination angle is given by

$$\delta = 23.45\sin(360 \cdot \frac{284+n}{365}) \tag{1}$$

The altitude angle, which is in the form of Sin, is obtained by

$$\sin(\alpha) = \sin(\varphi)\sin(\delta) + \cos(\varphi)\cos(\delta)\cos(\omega) \tag{2}$$

Where,

$$\omega = 15^{\circ} \cdot (\mathrm{t} - 12) \tag{3}$$

Where,

$$t = t_{st} + E/60 - 15 \times (L_{\mathrm{st}} - L_{loc}) \tag{4}$$

Where, L_{st} is 120°, i.e. longitude of Beijing, in China. And E is given by

$$E = 9.87\sin(2B) - 7.53\cos(B) - 1.5\sin(B) \tag{5}$$

Where,

$$B = \frac{360(n-81)}{364} \tag{6}$$

According to Kasten experienced equation [12], the solar air mass is given by

$$\mathrm{m} = \frac{1}{\sin(\alpha) + 0.15(\alpha + 3.885)^{-1.253}} \tag{7}$$

With the method of MO-1 [13], the coefficient of atmospheric transpareney is obtained by

$$P = P_2(\frac{\mathrm{m}}{2})^{-(\lg P_2 + 0.009)/1.547} \tag{8}$$

The solar irradiance of exoatmospheric tangential plane is given by

$$G_0 = \gamma G_{sc} \sin(\alpha) \tag{9}$$

Where,

$$\gamma = 1 + 0.033\cos(\frac{2\pi n}{365}) \tag{10}$$

According to **Eq.1-Eq.10**, the solar direct irradiance and diffuse irradiance through the atmosphere can be obtained by **Eq.11** and **Eq.12** respectively.

$$G_n = G_0 P^m = \gamma G_{sc} \sin(\alpha) P^m \tag{11}$$

$$G_{\mathrm{d}} = \frac{1}{2}\gamma G_{sc} \frac{1 - P^m}{1 - 1.4\ln P} \sin(\alpha) \tag{12}$$

With focus on impacts of grid-connected PV systems on voltage profiles, this paper assumes that voltage would not cross limit when at night. Thus, sunrise time and sunset time should be calculated as follows:

$$\mathrm{t}_{rise} = 12 - \arccos(-\tan\delta\tan\varphi)/15 \tag{13}$$

$$\mathrm{t}_{\mathrm{set}} = 12 + \arccos(-\tan\delta\tan\varphi)/15 \tag{14}$$

2.1.2 Solar irradiance on the inclined PV arrays

The solar irradiance on the inclined PV arrays concerns with weather, pollutant in the air, dust on the arrays, et al. The effect of weather will be elaborated in the next subsection. The effect of pollutant is so little that it is ignored. The dust could be washed away by rain and self surface cleaning solar panels appear presently, so dust is also out of consideration. Then, solar irradiance on the inclined PV arrays is given by

$$G = G_n R_b + G_d(\frac{1+\cos(\beta)}{2}) + (G_n + G_d)\rho\left(\frac{1-\cos(\beta)}{2}\right) \tag{15}$$

Where,

$$R_b = \cos(\theta)/\sin(\alpha) \tag{16}$$

Where, due to the PV arrays usually fixed due south in China, we have

$$\cos(\theta) = \sin(\delta)\sin(\varphi - \beta) + \cos(\varphi - \beta)\cos(\delta)\cos(\omega) \tag{17}$$

2.1.3 The effect of random change of weather

The random change of weather is caused by clouds in reality. The clouds may develop, dissipate or vary from one kind to another due to the change of meteorology. Different kinds of clouds have different impacts on PV systems. Since it is hard to get the information of variable clouds, the weather becomes the study point instead of clouds. According to the analysis of probability statistics, the variation of weather follows some rule that every transformation of state is based on the last state and independent of previous states, which could be taken as Markov stochastic process [14]. Thus we could use Markov transition probability matrix to describe it [15]. According to the variation of clouds, the weather could be divided into sun day, cloudy day, overcast sky, rain and snow for simplified analysis, and the Markov state transition diagram of them is presented in **Figure 1**.

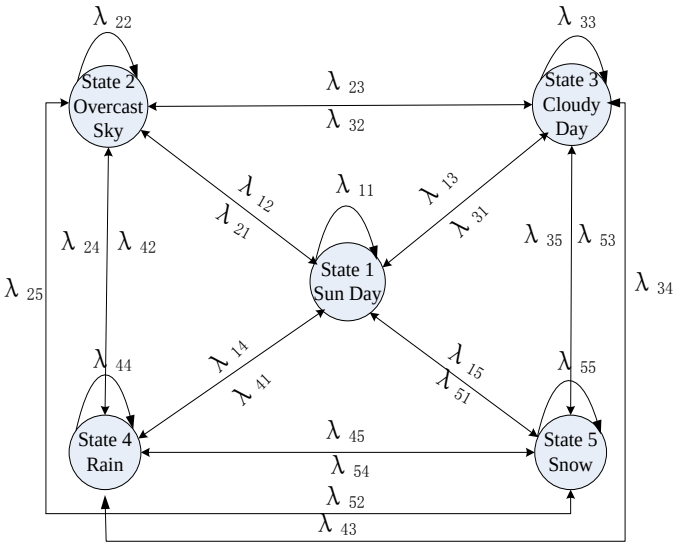

Figure 1. State transition diagram of weather

The transition probability (times in one month) between two states can be achieved according to historical data of weather. Assuming that the present state of weather is i, it needs to determine the next state and the transition time, which can be done as follows. Giving the present time t_1, the state transition probability between present weather and the five states is λ_{ij}, then, the transition time t_{ij} is obtained by

$$\mathrm{t}_{ij} = \frac{t_{base}}{\lambda_{ij}} \times U \quad (j = 1,2,3,4,5) \tag{18}$$

Where, j is the next probabilistic state; t_{base} is the number of hours of each month (e.g. months of 30 days are 720 hours; February is 672 hours, and left are 744 hours).

The least value $\mathbf{t_{min} = Min\ (t_{ij})}$ is the desired transition time and the corresponding j is the next transition state. In this way, the sustained time sequence of different weather can be obtained and hourly state can be acquired via sequential sampling. Next, supposing solar irradiance is unit on sun day, the attenuation coefficient (ξ) of solar irradiance in different weather for each hour can be obtained based on the analysis of historical data of solar irradiance. At last, the solar irradiance on PV arrays for each hour is given by

$$G_s = G \cdot \xi \tag{19}$$

2.2. The Efficiency of PV Cells

The conversion efficiency of PV cells is influenced by the

temperature of PV cells. The change of temperature involves wind speed and wind direction, but it is hard to quantify the relationships. Thus, the wind is assumed to be irrelevant in this paper and the temperature of PV cells is gained by hourly air temperature and solar irradiance.

The hourly air temperature is determined by weather. The hourly state of weather in every day is decided by weather sampling and the whole day's weather is the state that lasts the longest time on daytime. Next, it needs to decide the day's highest temperature T_{max} and lowest temperature T_{min} according to historical data of typical weather and then the temperature for each hour is obtained by

$$T_a(t) = \frac{1}{2}\left[T_{\max} + T_{\min} + (T_{\max} - T_{\min})\sin\frac{2\pi(t - t_p)}{24}\right] \quad (20)$$

Where, t_p is the time when the highest temperature occurs, taking it as 14:00 generally.

The temperature of PV cells is given by

$$T = T_a + 0.03G_s \quad (21)$$

Then the efficiency of PV cells is given by

$$\eta = \eta_0\left[1 - \varepsilon(T - T_r)\right] \quad (22)$$

2.3. The Effective Sun Light Area of PV Arrays

The back arrays, except the first row, may be affected by the shadow of the front arrays with the motion of sun, so the effective sun light area should be calculated.

As shown in **Figure 2**, x is the length of shadow and is obtained by following expressions.

$$H = L\sin(\beta) \quad (23)$$

$$d' = d - L\cos(\beta) \quad (24)$$

$$x = \frac{H - d'\tan(\alpha)}{\tan(\alpha)\cos(\beta) + \sin(\beta)} \quad (25)$$

The ratio of shadow is given by

$$P_s = \frac{x}{L} \quad (26)$$

Then the effective sun light area can be obtained by

$$S = W \times L + W \times L \times (R-1) \times (1 - P_s) \quad (27)$$

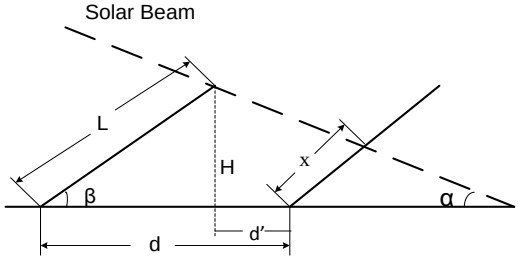

Figure 2. Schematic diagram of photovoltaic arrays shadow

2.4. The Output Power of Grid-connected PV System

Considering the efficiency of MPPT and inverter, the output power of PV system is given by

$$P_{pv} = \eta S G_s \eta_{mppt} \eta_{inv} \quad (28)$$

For grid-connected PV system, when the output power is lower than q% of rated power, the system should be separated from distribution networks. It keeps to the criterion that when P_{PV} is bigger than $\mathbf{P_N \cdot q\%}$, the PV system operates normally and the output is P_{PV}; otherwise, the PV system closes and the output is zero.

2.5. Reliability Sampling of Grid-connected PV System

In this paper, the reliability of PV system is also considered in simulation. Taking the PV system as a whole when studying the reliability parameters (i.e. fault rate and repair rate), because it is not easy to get the reliability parameters of PV arrays, inverter and filter respectively [16]. In simulation the state of whole grid-connected PV system is gained by sequential sampling. The run time and repair time are given by following equations.

$$T_{\text{run}} = \frac{8760}{\lambda_{pv}} \cdot U_1 \quad (29)$$

$$T_{\text{repair}} = \frac{8760}{\mu_{pv}} \cdot U_2 \quad (30)$$

When the system is in fault, the output is zero, else the output is P_{PV}.

3. Three-Phase Probabilistic Load Flow in Distribution System with Grid-Connected Pv Systems

3.1. Load Model

The time-varying load model [17] is used and the randomness of loads is considered in this paper. The load P_L of each hour is assumed to follow normal distribution [1]. The PDF of P_L is given by the following expression:

$$f(P_L) = \frac{1}{\sigma\sqrt{2\pi}} \cdot e^{\frac{-(P_L - \bar{P}_L)^2}{2\sigma^2}} \quad (31)$$

Where, $\bar{P}_L$ is mean value; σ is standard deviation.

3.2. Three-phase Load Flow

The forward/backward substitution method [18] is used to solve three-phase load flow. It includes following steps:

1) Read data of distribution system.
2) Initialize voltage in the network.
3) Calculate injected current at nodes.
4) Sum up line section current via forward sweep.

5) Update voltage via backward sweep.

6) Repeat iteration of 3) to 5) until the convergence criteria are satisfied.

7) Finish the calculation.

Here, assuming that the grid-connected PV systems operate with constant power factor (PF), so they are considered as PQ-type nodes in load flow analysis.

3.3. Probabilistic Load Flow

The authors developed a program to solve three-phase PLF in distribution system with three-phase and single-phase grid-connected PV systems based on the simulation method presented above, with the help of VC++ software. The loads and PV generator productions are assumed to be mutually independent. Variations of load flow and voltage profiles within a day can be achieved by year or month or day simulation in this program. Taking the day type for example, the main program flow chart is shown in **Figure 3**.

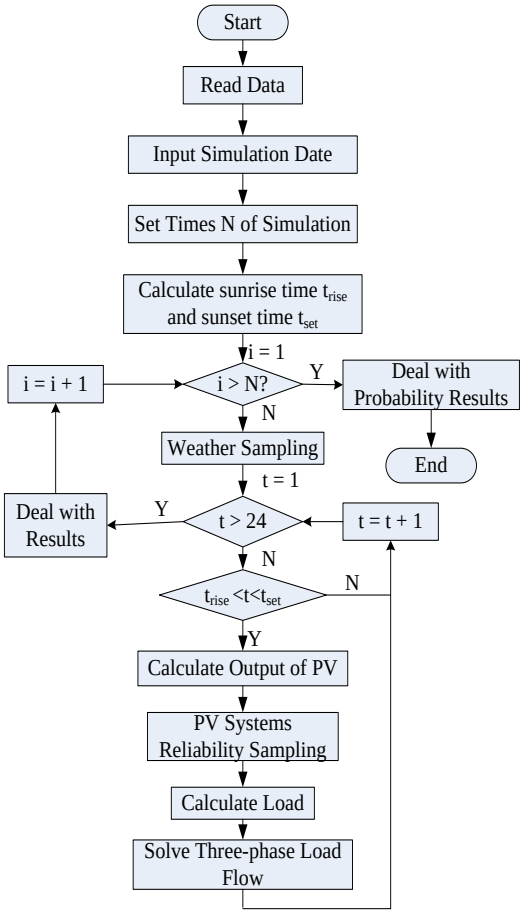

Figure 3. Main program flow chart of day type

4. Case Study

The IEEE 33-node distribution system, as shown in **Figure 4**, is analyzed in this section, given the terminal voltage 10.5kV. Three phase parameters of the network are modified to be unsymmetrical, which are introduced in [18].

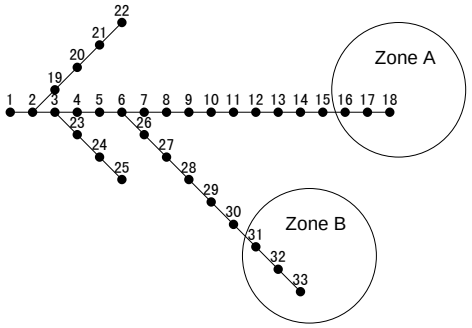

Figure 4. IEEE 33-node distribution system

4.1. Explanation For Cases

1) This paper assumes that PV installation site is Hefei (Anhui Province, China), whose latitude is 31.86° N and longitude is 117.27° E, , taking the day type for example. The simulation date is May 30th, on which the sunrise time is 5:07 and sunset time is 19:03. The time have been transformed to Beijing time.

2) Weather data needed are from local meteorological department. The PF of grid-connected PV systems are unit and other parameters for PV systems are not given in this paper due to space limit.

3) The power of single-phase PV system at 10kV node is assumed to be the sum of the power of each single-phase PV system owned by low-voltage consumers that are connected to this 10kV node through transformers.

4) The normal voltage of single phase in 10kV distribution system is limited between 9kV and 10.7kV in China. When outside the limit, we take it as voltage beyond limit.

5) Voltage imbalance is discussed in cases. Based on Chinese GB/T15543, the NSVUF at grid-connected node should be less than 2% for three-phase PV systems. In cases, the NSVUF is calculated by

$$VUF = \left| \frac{V_-}{V_+} \right| \times 100\% \tag{32}$$

Where, V_- and V_+ are amplitudes of negative sequence voltage and positive sequence voltage respectively.

6) Weather difference in different zones is considered in cases. As shown in **Figure 4**, if zone A is near zone B, the weather in them changes synchronously, thus output power of PV systems in them change with the same step, i.e., they are correlated. Otherwise, the output powers of PV systems are uncorrelated in zone A and B.

4.2. Cases Design and Result Analysis

Different cases are designed in order to verify the feasibility of the proposed method and study the impact of grid-connected PV systems on load flow in distribution system. The main points are the impacts of different types of grid-connected PV systems as well as the correlation of weather on voltage, since voltage quality is primarily

significant in distribution system. The number of simulations is 10000 in order to gain accurate result in each case.

Case 1: no grid-connected PV system, which is the base of the following comparison.

When the weather is perfectly correlated in zone A and B,

Case 2: there are there-phase PV systems rated 300kW at node 16, 17, 18, 31, 32, 33;

Case 3: there is another single-phase PV system rated 100kW connected to phase A at above six nodes respectively based on case 2;

Case 4: there is another single-phase PV system rated 100kW connected to phase B at above six nodes respectively based on case 3.

When the weather is uncorrelated in zone A and B, repeat case 2, case 3 and case 4, which are defined as case 5, case 6 and case 7 respectively.

The analysis of results just reported power flow of phase A in line 17-18 and voltage profiles of node 18 for the sake of brevity, since other lines or nodes can be analyzed in a similar way.

The variations of mean value of active power and reactive power of phase A in line 17-18 in case1 and case2 are presented in **Figure 5**. It can be noted that after integration of PV systems the direction of active power is changed from 7:00 to 17:00 and the amplitude of reverse flow increase first up to highest at noon and then decrease, but the direction is normal in the early morning and at dusk. Meanwhile, the reactive power keeps constant nearly whether PV systems are connected to the network or not, because the PF of PV systems are unit, i.e., the output reactive power of PV systems into the grid is zero.

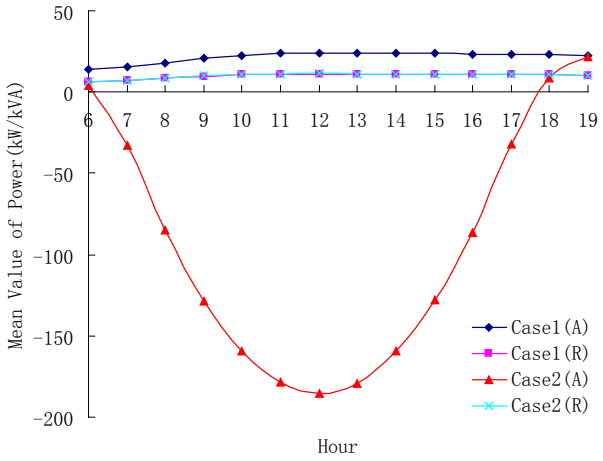

Figure 5. Variation of mean value of active power and reactive power of phase A in line 17-18. (A: active power; R: reactive power)

The variations of average voltage of each phase at node 18 are shown in **Figure 6**, **Figure 7** and **Figure 8**, in which 10.7kV is the upper limit of voltage. They indicate following points. Firstly, node voltages are improved with grid-connected PV systems and single-phase PV systems would improve the voltage further of phase to which the single-phase PV systems are connected. Secondly, node voltages become higher first and then decrease with integration of PV, and the highest values occur at noon. Thirdly, under the same grid-connected condition, when the weather is correlated the average voltage is lower than that when uncorrelated at the same time, which is obvious around noon.

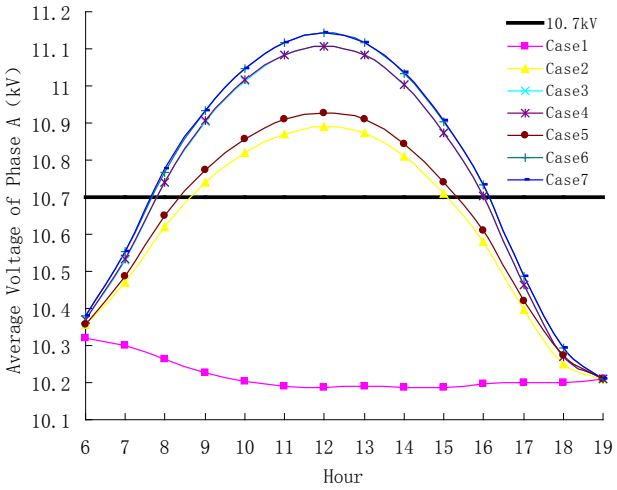

Figure 6. Variation of average voltage of phase A at node 18

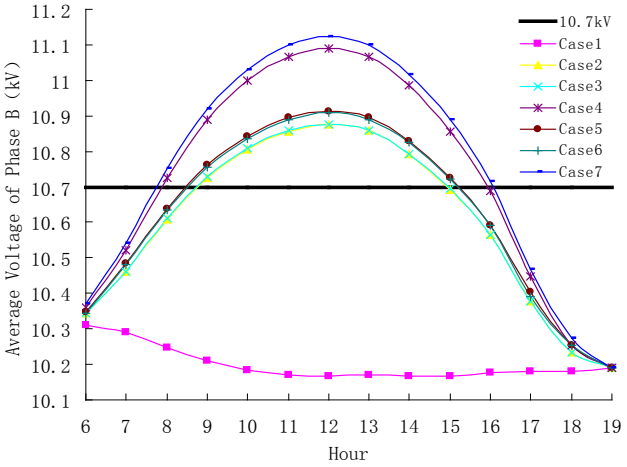

Figure 7. Variation of average voltage of phase B at node 18

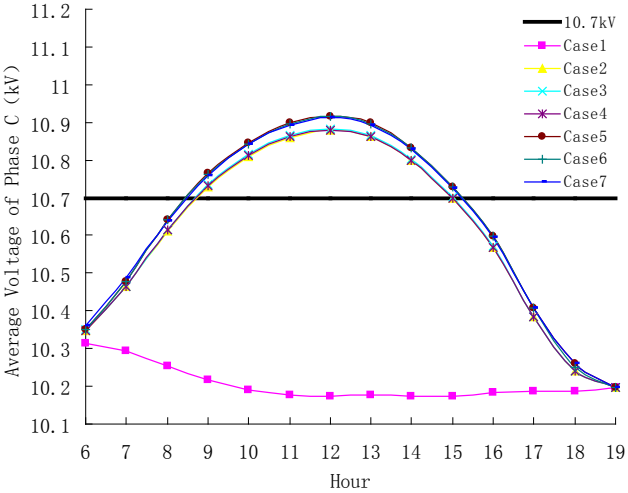

Figure 8. Variation of average voltage of phase C at node 18

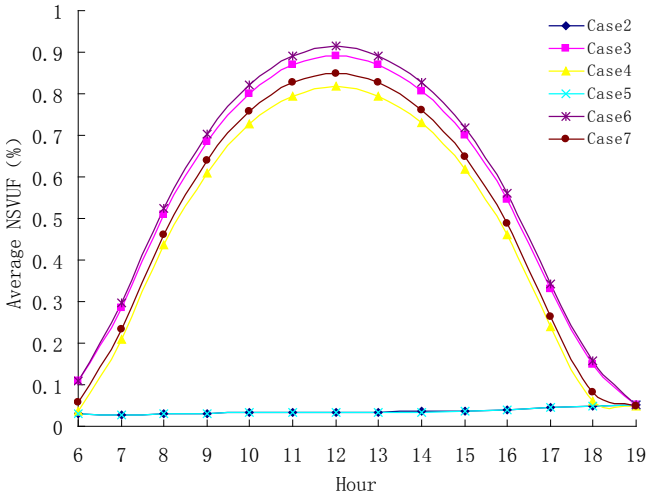

Figure 9. Variation of average NSVUF at node 18

The variation of average NSVUF at node 18 is presented in **Figure 9**. It indicates points as follows. Firstly, the NSVUF is small and varies little when there are only three-phase PV systems connected to the network on daytime, but it becomes bigger and increases first and then decreases when single-phase PV systems are added. Secondly, keeping the capacities of single-phase PV systems constant, the NSVUF is bigger when there is only one phase with single-phase PV systems than that when there are two phases with single-phase PV systems. Thirdly, under the same grid-connected condition, when the weather is correlated the NSVUF is smaller than that when uncorrelated at the same time.

Table.1 presents the probabilisties of each phase voltage beyond limit at node 18, in which the time when no voltage is beyond limit are removed. It shows following points. Firstly, the probabilities of each phase voltage beyond limit increase first and then decrease, and are up to highest at noon. Secondly, the probabilities beyond limit of phase with single-phase grid-connected PV systems are bigger than that of other phases. Thirdly, under the same grid-connected condition, the probabilities of each phase voltage beyond limit are smaller when the weather is correlated than that when uncorrelated at the same time, but the result is opposite if no single-phase grid-connected PV system connected to the network when the solar irradiation is weak, such as 8:00 and 16:00.

Table 1. Variation of probabilities of voltage beyond limit of each phase at node 18

Hour		8	9	10	11	12	13	14	15	16
Case2	A	0.5338	0.5364	0.5364	0.5374	0.5384	0.5390	0.5390	0.5372	0.3082
	B	0.5292	0.5364	0.5364	0.5374	0.5384	0.5390	0.5390	0.5372	0.3082
	C	0.5338	0.5364	0.5364	0.5374	0.5384	0.5390	0.5390	0.5372	0.3082
Case3	A	0.3694	0.6412	0.7042	0.7542	0.7546	0.7552	0.7016	0.5672	0.2494
	B	0.3112	0.5918	0.7038	0.7542	0.7546	0.7552	0.7016	0.5110	0.2438
	C	0.3120	0.6162	0.7040	0.7542	0.7546	0.7552	0.7016	0.5110	0.2490
Case4	A	0.5502	0.5490	0.7982	0.7980	0.7976	0.7974	0.7974	0.5480	0.5484
	B	0.5190	0.5484	0.5492	0.5488	0.5478	0.5482	0.5472	0.5472	0.2974
	C	0.5178	0.5484	0.5492	0.5488	0.5478	0.5482	0.5472	0.5472	0.2974
Case5	A	0.5574	0.6932	0.8594	0.9160	0.9166	0.9166	0.8170	0.6972	0.5574
	B	0.3076	0.5794	0.6926	0.7564	0.7574	0.7576	0.6952	0.5064	0.2312
	C	0.3152	0.6108	0.6926	0.7564	0.7574	0.7580	0.6952	0.5066	0.2456
Case6	A	0.5502	0.5490	0.7982	0.7980	0.7976	0.7974	0.7974	0.5480	0.5484
	B	0.5502	0.5490	0.7982	0.7980	0.7972	0.7972	0.7970	0.5480	0.5478
	C	0.5478	0.5484	0.5492	0.5488	0.5478	0.5482	0.5472	0.5472	0.2974
	A	0.5574	0.6932	0.8608	0.9160	0.9166	0.9166	0.8170	0.6972	0.5574

Case7	B	0.5568	0.6932	0.8148	0.9158	0.9158	0.9162	0.8166	0.6968	0.5588
	C	0.3152	0.5820	0.6926	0.7564	0.7574	0.7580	0.6952	0.5066	0.2432

5. Conclusions

A method has been proposed for three-phase PLF in distribution system with grid-connected PV systems using the technique of sequential Monte Carlo simulation, considering the stochastic nature of PV generation and loads. In the case of PV generation, probabilistic model of output power of grid-connected PV system is presented in detail. Based on the method, a relevant program is developed. Some cases have been implemented using the program to study the impacts of different types of grid-connected PV systems and weather correlation on the voltage. The conclusions from results of cases can be drawn as follows:

1) The proposed three-phase PLF method is feasible in unsymmetrical distribution system with different types of PV systems and it can express the time-sequence change of load flow due to hourly probabilistic output power of grid-connected PV systems.

2) PV generation may change the direction of power flow in distribution system, which would give rise to problems of control and operation.

3) Different types of grid-connected PV systems have different impacts on the node voltages of each phase in distribution system. It had better to avoid that there is too big difference in capacities of single-phase PV systems connected to each phase in order to decrease the NSVUF.

4) It is also suggested that PV systems with high penetration should be connected to the distribution system in the same zone, which is helpful to decrease the probability of voltage beyond limit as well as the NSVUF.

6. Acknowledgments

This work is supported by National Natural Science Foundation of China under Grant 50837001.

References

[1] Conti, S., Raiti, S., 2007. Probabilistic load flow using Monte Carlo techniques for distribution networks with photovoltaic generators. Solar Energy 81 (12), 1473-1481.

[2] Thomson, M., G.Infield, D., 2007. Impact of widespread photovoltaic generation on distribution systems. IET Journal of Renewable Power Generation 1 (1), 33-40.

[3] Hu, B., Nonkak, Y., Yokoyama, R., 2012. Influence of large-scale grid-connected photovoltaic system on distribution networks. Automation of Electric Power System 36 (3), 34-39.

[4] Eltawil, M. A., Zhao, Z., 2010. Grid-connected photovoltaic power systems: technical and potential problems – A review. Renewable and Sustainable Energy Reviews 14 (1), 112-129.

[5] Wang, C., Zheng, H., Xie Y., et al, 2005. Probabilistic power flow containing distributed generation in distribution system. Automation of Electric Power System 29 (24), 39-44.

[6] Zhang, Z., Li, G., Wang, S., Wang, J., Wang, Z., 2011. Stochastic evaluation of voltage in distribution networks considering the characteristic of distributed generators. International Conference on Electric Utility Deregulation and Restructuring and Power Technologies, 1132-1137.

[7] Saad, Y. E., Ponnambalam, K., El-Shatshat, R.A., 2010. Stochastic analysis of a local distribution company voltage profile under uncertain engery supply from a photovoltaic system. International Conference on European Energy Market, 1-7.

[8] Tina, G.., Gagliano, S., Raiti, S., 2006. Hybrid solar/wind power system probabilistic modeling for long-term performance assement. Solar Engrey 80 (5), 578-588.

[9] Fang, R., Wu, S.,. Wan, Y., Han, M., 2011. The analysis of distribution system with photovoltaic system generation based on probabilistic power flow. Asia-Pacific Power and Energy Engineering Conferece.

[10] Ruiz-Rodriguez, F.J., Hernandez, J.C., Jurado, F., 2012.Probabilistic load flow for radial distribution networks with photovoltaic generators. IET Renewable Power Generation 6 (2), 110-121.

[11] Yu, K., Cao, Y., Chen X., et al., 2011. Dynamic probability power flow of district grid containing distributed generation. Proceedings of the CSEE 31 (1), 20-25.

[12] Liu, J., Principle, 2010. Technique and Engineering of Solar Energy Utilization. Electronic Industry Press, Beijing.

[13] Ohvril, H., Okulov, O., 1999. The atmospheric integral transparency coefficient and the forbes effect. Solar Energy 66(4), 305-317.

[14] Claudia, V. T.,. Valria Tvora Cabral, D. O. Filho, et al., 2010. A stochastic method for stand-alone photovoltaic system sizing. Solar Energy 84 (9), 1628-1636.

[15] Billinton, R., Sc., D., Cheng, L., Sc., M., 1986. Incorporation of weather effects in transmission system models for composite system adequacy evaluation. IEE PROCEEDINGS 133 (6), 319-327.

[16] Tang, J., Huang, M., Jing W., et al., 2011. Reliability evaluation of distribution networks with grid-connected photovoltaic system. East China Electric Power 39 (2), 266-270.

[17] Grigg, C., Wong, P., ET AL., 1999. The IEEE Reliability Test System-1996 (A report prepared by the Reliability Test System Task Force of the Application of Probability Methods Subcommittee). IEEE Transactions on Power Systems 14 (3), 1010-1020.

[18] Ding, M., Guo, X., 2009. Three-phase power flow for the weakly meshed distribution network with the distributed generation. Proceedings of the CSEE 19 (13), 35-40.